# Characterizing the effects of shaking intensity on the kinetics of metallic iron dissolution in EDTA

Noubactep C.

Angewandte Geologie, Universität Göttingen, Goldschmidtstraße 3, D - 37077 Göttingen, Germany.

e-mail: cnoubac@gwdg.de; Tel. +49 551 39 3191, Fax: +49 551 399379

**Abstract**:

Despite two decades of intensive laboratory investigations, several aspects of contaminant removal from aqueous solutions by elemental iron materials (e.g., in $Fe^0/H_2O$ systems) are not really understood. One of the main reasons for this is the lack of a unified procedure for conducting batch removal experiments. This study gives a qualitative and semi-quantitative characterization of the effect of the mixing intensity on the oxidative dissolution of iron from two $Fe^0$-materials (material A and B) in a diluted aqueous ethylenediaminetetraacetic solution (2 mM EDTA). Material A (fillings) was a scrap iron and material B (spherical) a commercial material. The $Fe^0/H_2O$/EDTA systems were shaken on a rotational shaker at shaking intensities between 0 and 250 $min^{-1}$ and the time dependence evolution of the iron concentration was recorded. The systems were characterized by the initial iron dissolution rate ($k_{EDTA}$). The results showed an increased rate of iron dissolution with increasing shaking intensity for both materials. The increased corrosion through shaking was also evidenced through the characterization of the effects of pre-shaking time on $k_{EDTA}$ from material A. Altogether, the results disprove the popular assumption that mixing batch experiments is a tool to limit or eliminate diffusion as dominant transport process of contaminant to the $Fe^0$ surface.

**Keywords**: Co-precipitation, EDTA, corrosion products, Reactivity, Zerovalent iron.

## Introduction

Iron-based alloys (metallic iron, elemental iron or $Fe^0$ materials) have been used as an abiotic contaminant reducing reagent for organic and inorganic groundwater contaminants for over 15 years [1–13]. In this context, $Fe^0$ materials are widely termed as zerovalent iron (ZVI) materials, contaminants have been denoted as reductates [14], and the bare surface of $Fe^0$ as reductant. The reducing capacity of metallic iron is due to the low standard reduction potential of the redox couple $Fe^{II}/Fe^0$ ($E^0$ = -0.440 V). This makes $Fe^0$ a potential reducing agent relative to several redox labile substances, including hydrogen ions ($H^+$) and oxygen ($O_2$) [1,15].

Since contaminant reduction by $Fe^0$ materials is believed to be surface-mediated, increasing the surface area of the iron, for instance by increasing the amount of $Fe^0$ or decreasing the particle size, is believed to increase the rate of the reductive decontamination at the surface of $Fe^0$ [15,16]. Based on this seemingly logical premise mechanistic removal studies by $Fe^0$ materials have shown that the rate-determining step is electron transfer to the surface-adsorbed molecule [1,17]. There are several arguments against quantitative contaminant reduction at the $Fe^0$ surface; among others the following [18]:

(i) Huang et al. [19] observed a lag time of some few minutes at pH 4 before nitrate ($NO_3^-$) reduction took place. The experiments were conducted with 20 $g.L^{-1}$ $Fe^0$ (powder) and the solutions were shaken at 210 $min^{-1}$. During these “few minutes” the pH may have increased to values > 5 yielding iron oxide precipitates. Iron oxides adsorb $Fe^{II}$ (so called structural $Fe^{II}$) and $NO_3^-$ such that the observed $NO_3^-$ reduction may be mediated by structural $Fe^{II}$. Clearly, the lag time can be seen as the time necessary for reactive species to be produced.

(ii) The aqueous corrosion science has unequivocally shown that at pH > 5 the iron surface is always covered by an oxide film. In this regard Holmes and Meadowcroft [20] described an interesting thumbnail sketch in which without the protective action of a fence (oxide-film) the rabbit ($Fe^0$ surface) is a defenceless prey for a rapacious dog (corroding environment). The

oxide film generated by corroding $Fe^0$ is primary porous. Therefore, $Fe^0$ still corrodes after the formation of a surface film. This property is the main characteristic making $Fe^0$ materials suitable for environmental remediation.

The presentation above shows clearly that, while "putting corrosion to use" [21], an essential aspect of the iron corrosion was overseen. The main reason for this mistake is that, from the pioneer works on [1,2,17], the reaction vessels have been mixed with the justifiable intention to limit diffusion as transport mechanism of contaminant to the $Fe^0$ surface. However, mixing inevitably increases iron corrosion and depending on the mixing type and the mixing intensity, mixing may avoid/delay the formation of oxide films and/or provoke their abrasion.

The present study investigates the effect of mixing speed on the kinetics of iron dissolution in a system $Fe^0/H_2O/O_2$/EDTA (simply $Fe^0$/EDTA) while the shaking speed varies from 0 to 250 $min^{-1}$. In this system, $Fe^0$ is oxidized by dissolved $O_2$; resulted $Fe^{II}$ and $Fe^{III}$ species are complexed by EDTA. The reactivity of the $Fe^0$ material is mainly characterised by the dissolution rate ($k_{EDTA}$ in $\mu g.h^{-1}$ or $mg.h^{-1}$) deduced from the linearity of the iron concentration vs. time curve. The background of this procedure is presented elsewhere [21]. To further characterize $Fe^0$/EDTA systems, a new parameter is introduced ($\tau_{EDTA}$). Per definition, $\tau_{EDTA}$ for a given system is the time required for the iron concentration to reach 2 mM (112 mg/L). That is the time to achieve saturation assuming 1:1 complexation of $Fe^{II,III}$ by EDTA. To properly characterize the effects of the shaking intensity on the kinetics of iron dissolution ($k_{EDTA}$ and even $\tau_{EDTA}$), two $Fe^0$ materials of markedly different reactivity were selected (material A and material B). Material A is a scrap iron from a metal recycling company ("Sorte 69" from Metallaufbereitung Zwickau, Germany) and material B is a commercially available material ("Hartgußstrahlmittel" from Würth, Germany).

**Rationale for use the aqueous $Fe^0$/EDTA/$O_2$ system**

Ethylenediaminetetraacetic acid (EDTA) is a chelating agent that has been used as extracting (dissolving) agent in environmental sciences for decades (ref. [22] and references therein).

The capacity of EDTA to induce and promote the dissolution of iron oxides through surface complex formation that enhance the detachment of the surface metal is well known [23-25]. The driving force for dissolution is the solubility of the oxide phase, which is enhanced by the formation of aqueous $Fe^{III}$EDTA complexes. Using this dissolution tool, the reactivity of $Fe^0$ materials can be characterized [21].

In investigating the processes of contaminant removal in $Fe^0/H_2O$ systems EDTA has been used by several researchers [26-29] at concentrations varying from 0 to 100 mM. Thereby, the main goal was to prevent iron oxide precipitation and therefore, eliminate concurrent contaminant adsorption [27] or keep a clean iron surface for contaminant reduction [28]. EDTA was reported to both clean and passivate $Fe^0$ materials [26]. The extend and the time scale of occurring of both processes is surely a function of the used EDTA concentration [30]. In a recent study, Gyliene et al. [31] successfully tested $Fe^0$ as removing agent for aqueous EDTA.

In an effort to search for an effective, affordable, and environmentally acceptable method for chemical weapon destruction, the potential of the system "**z**erovalent iron, **E**DTA and **a**ir" (ZEA system) was recently investigated [32-34]. This system generates $HO^{\circ}$ radicals (in situ) for contaminant oxidation. The ZEA system has several advantages over other systems which have been investigated for the detoxification of organophosphorus compounds (e.g. hydrolysis, palladium-based catalysis, chemical oxidation). Because the ZEA reaction uses inexpensive reagents and proceeds in aqueous solutions, at room temperature and under atmospheric pressure, it can be performed in any laboratory.

This study aims at investigating the short-term kinetics of iron dissolution in ZEA systems while characterizing the effects of shaking intensity on this process. Clearly, a well documented methodology is used to characterize $Fe^0$ reactivity as influenced by the shaking intensity. In this method dissolved oxygen is a reactant and not a disturbing factor.

Furthermore since the investigations are limited to the initial phase of iron dissolution, the possibility that EDTA alters the corrosion process is not likely to be determinant.

## Experimental Section

### Materials

The used iron materials (material A and material B) were selected from 18 materials because of their different reactivity after the EDTA-test [21]. Material A is a scrap iron from a metal recycling company (Metallaufbereitung Zwickau, Germany) containing apart from iron about 3.5% C, 2% Si, 1% Mn and 0.7% Cr. This material was crushed and the size fraction 1.0–2.0 mm was used without further pretreatment. Material B is a spherical (mean diameter = 1.2 mm) commercially available material from Würth (Germany). Material B contained apart from iron about 3.39 % C, 0.41 % Si, 1.10 % Mn, 0.105 % S, and 0.34 % Cr and was used as received. The specific surface areas were 0.29 $m^2.g^{-1}$ [35] for material A and 0.043 $m^2.g^{-1}$ [36] for material B respectively.

### Solutions

A standard EDTA solution (0.02 M) from Baker JT® (Germany) was used to prepare the working solution. A standard iron solution (1000 mg/L) from Baker JT® was used to calibrate the Spectrophotometer. The reducing reagent for $Fe^{III}$-EDTA was ascorbic acid. 1,10 orthophenanthroline (ACROS Organics) was used as reagent for $Fe^{II}$ complexation. All other chemicals ($NaHCO_3$, L(+)-ascorbic acid, L-ascorbic acid sodium salt, and sodium citrate) used in this study were of analytical grade and all solutions were prepared using Milli-Q purified water.

### Iron dissolution experiment

Iron dissolution was initiated by the addition of 0.2 g of the $Fe^0$ material to 100 mL of a 2 mM EDTA solution. The experiments were conducted at laboratory temperature (about 22 °C) in polypropylene Erlenmeyer flask (Nalgene®). The Erlenmeyer was placed on a rotary shaker and allowed to react at 0, 50, 100, 150, 200 and 250 $min^{-1}$. The aqueous iron concentration

was determined spectrophotometrically with the 1,10 orthophenanthroline method [37,38] using a device from Varian (Cary 50) and recorded as a function of time. The spectrophotometer was calibrated for iron concentration ≤ 10 mg/L. Working EDTA-solution (0.002 M) was obtained by one step dilution of the commercial standard.

At various time intervals, 0.100 to 1.000 mL (100 to 1000 μL) of the solution (not filtrated) were withdrawn from the Erlenmeyer flask with a precision pipette (micro-pipette from Brand®) and diluted with distilled water to 10 mL (test solution) in glass essay tubes with 20 mL graduated capacity (the resulted iron concentration was ≤ 10 mg/L). After each sampling, the equivalent amount of distilled water was added to the Erlenmeyer in order to maintain a constant volume.

**Dissolution of iron and in situ generated iron corrosion products**

To evidence the fact that shaking the reaction vessels yields increased corrosion products (e.g. $Fe_3O_4$), 0.2 g of material A was added to 50 mL deionised water and pre-shaken at 100 $min^{-1}$ for 0, 3, 6, 18, 30 and 48 hours (systems I, II, III, IV, V and VI respectively). Subsequently, 50 mL of an ascorbate buffer was added to the systems (resulting ascorbate concentration: 0.115 M or 115 mM), the systems were further shaken at 100 $min^{-1}$, and the time dependence of the evolution of iron concentration was characterized. Under the experimental conditions (pH 7.6) aqueous iron originates essentially from two sources: (i) reductive dissolution of corrosion products through ascorbate, and (ii) oxidative dissolution of $Fe^0$ through dissolved oxygen. Assuming a 1:1 complexation, the used ascorbate concentration can dissolve 115 mM of iron or 38 mM of magnetite ($Fe_3O_4$), that is 8.9 g of corrosion products. Because only 0.2 g of $Fe^0$ material (producing maximal 0.28 g of $Fe_3O_4$) was used for the experiments, ascorbate was necessarily in excess with respect to the possible amount of corrosion products. It is expected that the amount of dissolved iron will be minimal in the non-pre-shaken system (reference, pre-shaken for 0 hour) and increased with increasing pre-shaking time.

## Analytical methods

For iron determination, 1 mL of a 0.4 M ascorbate buffer was added to the test solution (10 mL) in the essay tube for $Fe^{III}$ reduction followed by two times 4 mL distilled water for homogenisation. Finally, 1 mL of a 1 % 1,10 phenanthroline solution was added for $Fe^{II}$ complexation. The serial addition of ascorbate buffer (1 mL), water (2 * 4 mL) and phenanthroline solution (1 mL) occurred with an appropriated device from Brand® (Handystep). The essay tubes were then sealed, vigorously shaken manually and allowed to react for at least 15 min. The iron concentration was determined at 510 nm on the Spectrophotometer. The kinetics of $Fe^0$ oxidative dissolution was investigated by determining the amount of iron in the supernatant solution. The experiments were performed in triplicates. The mean values are presented together with the standard deviation (bares in the figure).

## Results and Discussion

### Background

The present work characterises the effects of shaking speed on the rate of iron dissolution ($k_{EDTA}$) from two $Fe^0$-materials in a 0.002 M EDTA solution. Under the experimental conditions $Fe^0$ is oxidised by dissolved $O_2$ and resulted $Fe^{II}$ and $Fe^{III}$ species are complexed by EDTA. Ideally, under given experimental conditions, Fe concentration increases continuously with time from 0 $mg.L^{-1}$ at the start of the experiment (t = 0) to 112 $mg.L^{-1}$ (0.002 M) at saturation ($\tau_{EDTA}$) when a 1:1 complexation of Fe and EDTA occurs. During this period the initial uncoloured solution becomes increasingly yellow. After saturation is reached, Fe concentration may: (i) increase, turning the solution a darker brown colour, (ii) remain constant or (iii) decrease depending on the dominating processes in the bulk solution. For example, if the hydrodynamic conditions are favourable for super-saturation the aqueous iron concentration will increase. If the nucleation is favourable and rapid the iron concentration will decrease more or less rapidly. This study is mainly focused on processes occurring before the saturation. Thereby, the time-variant iron concentration is likely to be linear. The solutions

were not filtered and concentrations above saturation are regarded as being of indicative nature even though the results were reproducible. Clearly, reported iron concentrations may not necessarily reflected dissolved iron. However, it is the aim of this study to show that particulate or colloidal iron is produced by mixing and influence the accessibility of $Fe^0$.

**Results**

Figure 1 and table 1 summarize the results of the kinetics of iron dissolution from the used $Fe^0$ materials as the shaking speed varies from 0 to 250 $min^{-1}$. These experiments mostly lasted from 3 to 100 h at all mixing intensities.

The results from Fig. 1 can be summarized as follows.

- A 2 mM EDTA solution is efficient at sustaining $Fe^0$ (oxidative) dissolution at pH values > 5 (initial pH: 5.2).
- Fe dissolution in 2 mM EDTA is significantly increased by shaking the experimental vessels. The higher the shaking intensity, the higher the dissolution rate.
- The Fe dissolution from material A (Fig. 1a) may yield to Fe saturation at all tested shaking intensities (including 0 $min^{-1}$).
- Fe saturation for material B (Fig. 1b) was achieved only for a shaking intensity of 150 $min^{-1}$ (114 ± 7 $mg.L^{-1}$). For higher mixing intensities (200 and 250 $min^{-1}$) a maximal concentration of about 80 $mg.L^{-1}$ (70 % saturation) was reached. There was no significant difference between the experiments at 200 and 250 $min^{-1}$ indicating that increasing the mixing intensity from 200 to 250 $min^{-1}$ will not significantly affect material B reactivity.
- For both materials the initial dissolution ($k_{EDTA}$) was always a linear function of the time; the regression parameters from these functions are given in table 1.
- For mixing intensities > 150 $min^{-1}$ the linear part of the curve [Fe] = f(t); is practically parallel to the [Fe] axis. This yields to physically meaningless b values (table 1). [Fe] = $k_{EDTA}$*t + b. Ideally, b is the concentration of iron at origin. It is per definition the

204 amount of iron dissolved from atmospheric corrosion products, present on $Fe^0$ at the
205 beginning of the experiment [21].

206 The results from table 1 can be summarized as follows.

207 ❖ The dissolution rate ($k_{EDTA}$) for material A varies from 83 $\mu g.h^{-1}$ at 0 $min^{-1}$ (not
208 shaken) to 1970 $\mu g.h^{-1}$ (ca. 2 $mg.h^{-1}$) at 250 $min^{-1}$. For material B $k_{EDTA}$ varies from 52
209 $\mu g.h^{-1}$ at 50 $min^{-1}$ to 1070 $\mu g.h^{-1}$ (ca. 1 $mg.h^{-1}$) at 250 $min^{-1}$. This result shows that
210 material A is more reactive in a non-shaken experiment than material B shaken at 50
211 $min^{-1}$.

212 ❖ The same trend for $k_{EDTA}$ was observed for $\tau_{EDTA}$. The largest value of $\tau_{EDTA}$ (213
213 hours or 9 days) was observed for material B shaken at 50 $min^{-1}$ and the lowest for
214 material A at 250 $min^{-1}$ (4 hours). This observation demonstrates the ability of $\tau_{EDTA}$
215 to characterise the reactivity of $Fe^0$ material under various experimental conditions.

216 ❖ For mixing intensities ≤ 150 $min^{-1}$, $k_{EDTA}$ (Fig. 2), b-values and $\tau_{EDTA}$ linearly
217 increased with the mixing speed. A sudden change was observed between 150 and 200
218 $min^{-1}$ for both materials despite the huge reactivity difference (Fig. 2). This material-
219 independent behaviour suggests a change in the hydrodynamic regime. In
220 $Fe^0/H_2O$/contaminant systems, this region at higher mixing intensities is associated
221 with the absence of transport limitations (e.g. ref. [39]). However, considering the fact
222 that Fe oxyhydroxides precipitate in the system as well, it is possible that contaminant
223 removal at higher mixing intensities is associated with oxide precipitation and not with
224 the iron surface. This conclusion is supported by recent data on methylene blue
225 discoloration in $Fe^0/H_2O$ systems [40,41]. Several studies have concluded that $Fe^0$
226 transformation reactions are either transport limited [42-44] or reaction limited
227 [45,46]. Since an oxide film is always present on the $Fe^0$ surface (at pH > 5), diffusion

is an inevitable transport path. Moreover mechanistic investigations should be performed under conditions favouring diffusion [18].

**Discussion**

As shown above no Fe super-saturation occurs in experiments with material B. In all experiments with this material the solution at the end of the experiment was almost yellow and limpid. On the contrary yellow limpid solutions were observed as end-solutions in experiments with material A only at shaking speeds ≤ 150 $min^{-1}$. For experiments at 200 and 250 $min^{-1}$ a turbid dark-brown coloration was observed some hours after the start of the experiment. Table 2 summarizes some basic equations for corrosion product generation. Simplifying, the observed coloration can be considered as the result of a precipitation reaction between excess $Fe^{3+}$ ions (after solution saturation) from iron corrosion and $OH^-$ ions from $O_2$ reduction yielding $Fe(OH)_3$ precipitates (see Tab. 2, Eqs 13, 16, 17). Like all precipitation processes, this reaction is influenced by mixing. Mixing liquids to precipitate solid particles is a common multiphase chemical process that comprises several complex phenomena [47-57].

The reaction between $Fe^{3+}$ and $OH^-$ initially forms soluble $Fe(OH)_3$, but in a supersaturated, metastable state relative to its equilibrium solubility product. Comparing the behaviour of both materials it can be stated that the metastability is possible around a shaking speed of 150 $min^{-1}$. This statement is supported by the persistence of the yellow colour at an over-saturation of 70 % in the experiment with material A at 150 $min^{-1}$ ([Fe] = 188 ± 11 $mg.L^{-1}$ after 95 hours). Note that in the experiment with material B a mixing speed of 150 $min^{-1}$ was the only condition where saturation could be achieved. For shaking speeds > 150 $min^{-1}$, either heterogeneous or homogeneous nucleation may have produced stable nuclei that grow into precipitate particles, causing the super-saturation to decline toward its equilibrium value. This is the reason for brownish coloration in experiments with material A where the apparent over-saturation results from suspended particles rather than true super-saturation (the samples were

253 not filtered). In experiments with material B nucleation formation yielded to a stagnation of
254 Fe-concentration at a value of 80 mg/L.
255 If such a system is allowed to age, the increasing stable nucleus size leads to ripening,
256 coarsening of the particulate size distribution, by dissolution of the smallest particles and
257 transfer of their mass to the larger particles [56,58]. Owing to the low solubility of Fe
258 oxyhydroxides, in the absence of a complexing agent (pH > 5) all the processes enumerated
259 above occurred but solely in the vicinity of $Fe^0$ materials if the system remains undisturbed.
260 Indeed, mixing affects both the corrosion rate of the bare $Fe^0$ surface and the precipitation rate
261 of iron oxides [18]. Prior to any film formation, high mixing rates lead to increased corrosion
262 rates as the transport of cathodic species toward the $Fe^0$ surface is enhanced by turbulent
263 transport. At the same time, the transport of $Fe^{2+}$ ions away from the $Fe^0$ surface is also
264 increased, leading to a lower concentration of $Fe^{2+}$ ions at the $Fe^0$ surface. This results in a
265 lower surface super-saturation and slower precipitation rate. Both effects account for, that no
266 or less oxide-films are formed at high mixing rates [59].
267 The results of this study suggest that, while investigating several aspects of contaminant
268 removal by elemental iron, there will be a critical mixing speed (here 150 $min^{-1}$) above which
269 iron precipitation becomes so fast, that its rate becomes controlled by mixing [55,60]. Under
270 these conditions, segregating the reaction kinetics of the contaminant reductive removal
271 process from the processes associated with Fe oxyhydroxides precipitation (adsorption, co-
272 precipitation) is an impossible issue. Therefore, the argument of a reaction-limited domain at
273 higher mixing rates [37,39,60,61] is questionable. Even under mixing speeds where iron
274 precipitation is moderate, mixing accelerates iron corrosion while avoiding or delaying the
275 formation of corrosion products at the surface of $Fe^0$. This impact of mixing on $Fe^0$ materials
276 has been mostly overseen in investigations regarding $Fe^0$ for groundwater remediation.
277 It is interesting to notice that the observed effect of shaking speed on the $Fe^0$ reactivity is
278 qualitatively the same as the often-enunciated effect of mixing intensity on reaction rate

constant to demonstrate the possibility of mass transfer limitations for reactions with elemental metals in batch systems [39]. Thereafter, the overall rate of contaminant reduction by $Fe^0$ materials should be mass transfer-limited at slow mixing speeds and reaction-limited at higher mixing speeds. This generally assumed trend is not univocally accepted. As an example, Warren et al. [62] worked with $Fe^0$ and $Zn^0$ and came to the conclusion that the overall rate of reaction may have been mass-transfer limited in the experiments involving $Fe^0$, and reaction-limited in the $Zn^0$ experiments. Concordantly to the results of Warren et al. [62] (34) and evidences from the open corrosion literature [20,44,63-67], the results of the present study suggest that the rate of contaminant reduction by $Fe^0$ materials is always mass-transfer limited. Moreover, the reported reaction mechanism difference at slow and high mixing speeds is likely to be the result of the interference of iron precipitation on the removal process. The products of iron oxide precipitation, whether suspended or settled, necessarily participate to the process of contaminant removal from the aqueous phase. The next section will evidence the increased corrosion at a shaking speed of 100 $min^{-1}$.

**Evidence of increased corrosion through shaking**

The results above confirm the evidence that iron corrodes in water under stagnant and turbulent conditions. Figure 3 summarises the results of the evolution of dissolved iron in 0.115 M ascorbate as influenced by pre-shaking operations. It can be seen that the expected trend for the evolution of iron concentration was observed for all systems only for experimental durations > 12 hours. For t < 12 hours the kinetic of iron dissolution was not uniform. During this period, the evolution of iron concentration in systems IV and V was very comparable to that of the reference system, and systems II, III and VI exhibited lower iron dissolution kinetics. Figure 3a for instance shows the results for the reference system (system I) and the systems pre-shaken for 30 and 48 hours (systems V and VI). It can be seen that in the initial period of the experiment (t < 6 h), iron dissolution is minimal in system VI (48 h) and very similar in systems I (0 h) and V (30 h). This observation can be attributed to the

305 differential dissolution behaviour of atmospheric corrosion products (system I) and in-situ
306 generated corrosion products (systems V and VI) on the one side and the differential
307 dissolution behaviour of in-situ generated corrosions products as function of time. The
308 process of aqueous corrosion products generation is known to be complex. For the discussion
309 in this section, it is sufficient to consider that in system V (30 h) a part of corrosion products
310 has a dissolution rate comparable to that of atmospheric products, whereas in system V (48
311 hour) ripening and crystallisation processes may have stabilised some corrosion products,
312 making them more resistant to ascorbate dissolution. Another important behavioural aspect of
313 corrosion products is to limit the accessibility of the $Fe^0$ surface for dissolved oxygen [66].
314 From Fig. 3a, it can be seen that after about 12 hours, the evolution of the iron concentration
315 is a linear function of the time and that the lines for system I and V for example are almost
316 parallel. This result indicates that, after the reductive dissolution has freed the $Fe^0$ surface,
317 dissolved molecular $O_2$ oxidised $Fe^0$ uniformly. The distance between the lines of system I
318 and system V is a qualitative reflect of the amount of corrosion products generated during the
319 pre-shaking period. The solubility of the available corrosion products has to be considered as
320 well. This is the reason why more iron dissolved in system V (30 h) than in system VI (48 h).
321 Figure 3b shows the results of iron dissolution for alls five systems in comparison to the
322 reference system. The excess iron amount in μm $Fe_3O_4$ in the individual systems is given as
323 function of the elapsed time. As discussed above it can be seen that in the initial phase of the
324 dissolution experiment a more or less deficit exists (negative value of ΔFe) in all systems,
325 which is primarily attributed to the effects of corrosion products on the availability of $Fe^0$ for
326 dissolved $O_2$. For longer experimental durations, an increased corrosion products generation
327 is observed in all systems. The lack of monotone trend in this increase is attributed to the
328 complex processes accompanying the process of iron corrosion as discussed above.

## Concluding remarks

By quantifying iron oxidative dissolution in 2 mM EDTA under varying mixing speeds, this study has qualitatively evidenced a crucial operational shortcoming associated with the effort to limit the impact of mass-transfer while investigating the processes of contaminant removal by $Fe^0$ materials. In fact, irrespective from the presence of any contaminant, mass transfer of soluble corrosion products (primarily $Fe^{2+}$, $Fe^{3+}$ $OH^-$, $Fe(OH)_{2(aq)}$ and $Fe(OH)_{3(aq)}$) and their precipitation in flowing groundwater is a complex process. While focussing the attention of the behaviour of a selected group of contaminants, most of the existing studies on contaminant removal in $Fe^0/H_2O$ systems have felt to adequately consider the interference of corrosion products precipitation [$Fe(OH)_{2(s)}$ and $Fe(OH)_{3(s)}$]. The present study discusses the effects of mixing speed on the reactivity of $Fe^0$ materials and confirms available results from others branches of corrosion science [44,66], that contaminant removal studies should be performed in the mass transfer controlled regime. Ideally, this regime is achieved under static (non-disturbed) conditions.

Since stagnation is not expected in reactive walls, non-shaken batch experiments do not replicate practical situations. However, this experimental procedure offers a simple tool for the investigation of the impact of oxide-film formation on the contaminant transport to $Fe^0$ surface. Another promising experimental procedure was proposed by Devlin et al. [68] and involves the use of a glass-encased magnet reactor in a sealed beaker. In this procedure a granular $Fe^0$ sample remains stationary while the solution is stirred. In this manner, slowly stirring overcomes the kinetics of mass transfer while corrosion products are not swept from $Fe^0$ surface. By carefully selecting the stirring speed, real field conditions can be closely simulated.

In light of the results of this study, published results on several aspects of contaminant removal in $Fe^0/H_2O$ systems can be reviewed. Thereby, one should try to compare results obtained under comparable mixing regimes. For mechanistic investigations, only results

obtained in the mass transfer controlled regime should be considered. Furthermore, to facilitate comparison of experimental results, the intrinsic material reactivity should be characterised by using the introduced parameter ($\tau_{EDTA}$). In analogy to iodine number for activated carbon, $\tau_{EDTA}$ can be adopted as standard parameter for $Fe^0$ characterization. This parameter is facile to obtain, cost-effective and does not involve any stringent reaction conditions nor sophisticated laboratory devices. To complete investigations on the mixing effect on $Fe^0$ reactivity, other mixing types (stirring, bubbling, end-over-end rotating, ultrasonic mixing, vortex) and the impact of reactor geometry should be focussed on. The results of such concerted investigations could be critical $\tau_{EDTA}$ values (guide values) at which specific experiments have to be performed. For example, results of Noubactep et al. [41] suggested that, shaking intensities aiming at facilitating contaminant mass transfer to the $Fe^0$ surface using material A should not exceed 50 $min^{-1}$. Based on this result, $\tau_{EDTA} \leq 90$ h (3.75 d) can be adopted as a guide value for the investigation of mass transfer limited processes. For less reactive $Fe^0$ materials this critical $\tau_{EDTA}$ value will be achieved at shaking intensities > 50 $min^{-1}$, but necessarily $\leq$ 150 $min^{-1}$ as the hydrodynamics change at 150 $min^{-1}$ (Fig. 2). Establishing a small $\tau_{EDTA}$ database for the most currently used $Fe^0$ materials (Fluka filings, Baker chips, Fisher filings, G. Maier GmbH, ISPAT GmbH, Connelly-GPM) can be regarded as an important step toward a broad-based understanding of iron reactive wall technology.

**Acknowledgments**

Interesting discussions were held with Dr. T. Licha (Angewandte Geologie, Universität Göttingen) on the spectrophotometric iron determination with o-phenanthroline in the presence of EDTA and are kindly acknowledged. For providing the $Fe^0$ materials used in this study the author would like to express his gratitude to the branch of the Metallaufbereitung Zwickau Co in Freiberg (Germany) and Dr. R. Köber from the Institute Earth Science of the

University of Kiel. M. Rittmeier and R. Pfaar are kindly acknowledged for technical support. The work was supported by the Deutsche Forschungsgemeinschaft (DFG-No 626/2-1).

**References**

[1] L.J. Matheson, P.G. Tratnyek, Reductive dehalogenation of chlorinated methanes by iron metal, Environ. Sci. Technol. 28 (1994), 2045-2053.

[2] Gillham R.W., S.F O'Hannesin, Enhanced degradation of halogenated aliphatics by zero-valent iron. Ground Water 32 (1994), 958-967.

[3] S.F. O'Hannesin, R.W. Gillham, Long-term performance of an in situ "iron wall" for remediation of VOCs. Ground Water 36 (1998), 164-170.

[4] T. Bigg, S.J. Judd, Zero-valent iron for water treatment. Environ. Technol. 21 (2000), 661-670.

[5] M.M. Scherer, S. Richter, R.L. Valentine, P.J.J. Alvarez, Chemistry and microbiology of permeable reactive barriers for in situ groundwater clean up. Rev. Environ. Sci. Technol. 30 (2000), 363–411.

[6] J.L. Jambor, M. Raudsepp, K. Mountjoy, Mineralogy of permeable reactive barriers for the attenuation of subsurface contaminants. Can. Miner. 43 (2005), 2117-2140.

[7] A.D. Henderson, A.H. Demond, Long-term performance of zero-valent iron permeable reactive barriers: a critical review. Environ. Eng. Sci. 24 (2007), 401-423.

[8] D.F. Laine, I.F. Cheng, The destruction of organic pollutants under mild reaction conditions: A review. Microchem. J. 85 (2007), 183-193.

[9] A.B. Cundy, L. Hopkinson, R.L.D. Whitby, Use of iron-based technologies in contaminated land and groundwater remediation: A review. Sci. Tot. Environ. 400 (2008), 42-51.

[10] R.L. Johnson, R.B. Thoms, R.O'B. Johnson, T. Krug, Field evidence for flow reduction through a zero-valent iron permeable reactive barrier. Ground Water Monit. Remed. 28 (2008), 47-55.

405 [11] R.L. Johnson, R.B. Thoms, R.O'B. Johnson, J.T. Nurmi, P.G. Tratnyek, Mineral
406 precipitation upgradient from a zero-valent iron permeable reactive barrier. Ground Water
407 Monit. Remed. 28 (2008), 56-64.
408 [12] J. Suk O, S.-W. Jeen, R.W. Gillham, L. Gui, Effects of initial iron corrosion rate on long-
409 term performance of iron permeable reactive barriers: Column experiments and numerical
410 simulation. J. Contam. Hydrol. 103 (2009), 145-156.
411 [13] R. Thiruvenkatachari, S. Vigneswaran, R. Naidu, Permeable reactive barrier for
412 groundwater remediation. J. Ind. Eng. Chem. 14 (2008), 145-156.
413 [14] R. Miehr, P.G. Tratnyek, Z.J. Bandstra, M.M. Scherer, J.M. Alowitz, J.E. Bylaska,
414 Diversity of contaminant reduction reactions by zerovalent iron: Role of the reductate.
415 Environ. Sci. Technol. 38 (2004), 139-147.
416 [15] B. Schrick, J.L. Blough, A.D. Jones, T.E. Mallouk, Hydrodechlorination of
417 trichloroethylene to hydrocarbons using bimetallic nickel-iron nanoparticles. Chem. Mater 14
418 (2002), 5140-5147.
419 [16] Johnson T.L., Scherer M.M., Tratnyek P.G. (1996): Kinetics of halogenated organic
420 compound degradation by iron metal. Environ. Sci. Technol. 30, 2634-2640.
421 [17] E.J. Weber, Iron-mediated reductive transformations: investigation of reaction
422 mechanism. Environ. Sci. Technol. 30 (1996), 716-719.
423 [18] C. Noubactep, Processes of contaminant removal in "$Fe^0$–$H_2O$" systems revisited: The
424 importance of co-precipitation. Open Environ. J. 1 (2007), 9-13.
425 [19] C.-P. Huang, H.-W. Wang, P.-C. Chiu, Nitrate reduction by metallic iron. Wat. Res. 32
426 (1998), 2257-2264.
427 [20] D.R. Holmes, D.B. Meadowcroft, Physical methods in corrosion technology. Phys.
428 Technol. 8 (1977), 2-9.
429 [21] C. Noubactep, G. Meinrath, P. Dietrich, M. Sauter, B. Merkel, Testing the suitability of
430 zerovalent iron materials for reactive walls. Environ. Chem. 2 (2005), 71-76.

[22] J. Yu, D. Klarup, Extraction kinetics of copper, zinc, iron, and manganese from contaminated sediment using disodium ethylenediaminetetraacetate. Water Air Soil Pollut. 75 (1994), 205-225.

[23] H.-C. Chang, E. Matijevi, Interactions of metal hydrous oxides with chelating agents. IV. Dissolution of hematite. J. Colloid Interf. Sci. 92 (1983), 479-488.

[24] J. Rubio, E. Matijevi, Interactions of metal hydrous oxides with chelating agents. I. β-FeOOH—EDTA. J. Colloid Interf. Sci. 68 (1979), 408-421.

[25] J.E. Szecsody, J.M. Zachara, P.L. Bruckhart, Adsorption-dissolution reactions affecting the distribution and stability of $Co^{II}$EDTA in iron oxide-coated sand. Environ. Sci. Technol. 28 (1994), 1706-1716.

[26] T.L. Johnson, W. Fish, Y.A. Gorby, P.G. Tratnyek, Degradation of carbon tetrachloride by iron metal: Complexation effects on the oxide surface. J. Cont. Hydrol. 29 (1998), 379-398.

[27] A. Abdelouas, W. Lutze, H.E. Nutall, W. Gong, Réduction de l'U(VI) par le fer métallique: application à la dépollution des eaux. C. R. Acad. Sci. Paris, Earth Planetary Sci. 328 (1999), 315-319.

[28] J.-L. Chen, S.R. Al-Abed, J.A. Ryan, Z. Li, Effects of pH on dechlorination of trichloroethylene by zero-valent iron J. Hazard. Mater B83 (2001), 243-254.

[29] C. Noubactep, Effect of selected ligands on the U(VI) immobilization by zerovalent iron. J. Radioanal. Nucl. Chem 267 (2006), 13-19.

[30] E.M. Pierce, D.M. Wellman, A.M. Lodge, E.A. Rodriguez, Experimental determination of the dissolution kinetics of zero-valent iron in the presence of organic complexants. Environ. Chem. 4 (2007), 260-270.

[31] O. Gyliene, T. Vengris, A. Stonccius, O. Nivinskien, Decontamination of solutions containing EDTA using metallic iron. J. Hazard. Mater. 159 (2008), 446-451.

456 [32] C. Noradoun, M.D. Engelmann, M. McLaughlin, R. Hutcheson, K. Breen, A.
457 Paszczynski, I.F. Cheng, Destruction of chlorinated phenols by dioxygen activation under
458 aqueous room temperature and pressure conditions. Ind. Eng. Chem. Res. 42 (2003), 5024-
459 5030.
460 [33] C.E. Noradoun, I.F. Cheng, EDTA degradation induced by oxygen activation in a
461 zerovalent iron/air/water system. Environ. Sci. Tchnol. 39 (2005), 7158-7163.
462 [34] C.E. Noradoun, C.S. Mekmaysy, R.M. Hutcheson, I.F. Cheng, Detoxification of
463 malathion a chemical warfare agent analog using oxygen activation at room temperature and
464 pressure. Green Chem. 7 (2005), 426-430.
465 [35] C. Mbudi, P. Behra, B. Merkel, The Effect of Background Electrolyte Chemistry on
466 Uranium Fixation on Scrap Metallic Iron in the Presence of Arsenic. Paper presented at the
467 Inter. Conf. Water Pollut. Natural Porous Media (WAPO2), Barcelona (Spain) April 11 – 13
468 (2007), 8 pages.
469 [36] O. Schlicker, Der Einfluß von Grundwasserinhaltsstoffen auf die Reaktivität und
470 Langzeitstabilität von Fe0-Reaktionswänden. Dissertation, Univ. Kiel (1999) 101 pp.
471 [37] L.G. Saywell, B.B. Cunningham, Determination of iron: colorimetric o-phenanthroline
472 method. Ind. Eng. Chem. Anal. Ed. 9 (1937), 67-69.
473 [38] W.B. Fortune, M.G. Mellon, Determination of iron with o-phenanthroline: a
474 spectrophotometric study. Ind. Eng. Chem. Anal. Ed. 10 (1938), 60-64.
475 [39] S. Choe, Y.Y. Chang, K.Y. Hwang, J. Khim, Kinetics of reductive denitrification by
476 nanoscale zero-valent iron. Chemosphere 41 (2000), 1307-1311.
477 [40] C. Noubactep, Characterizing the Discoloration of Methylene Blue in $Fe^0/H_2O$ Systems.
478 J. Hazard. Mater. 166 (2009), 79-87.
479 [41] C. Noubactep, A.-M.F. Kurth, M. Sauter, Evaluation of the effects of shaking intensity
480 on the process of methylene 2 blue discoloration by metallic iron. J. Hazard. Mater.
481 Doi:10.1016/j.jhazmat.2009.04.046 (In Press).

[42] A. Agrawal, P.G. Tratnyek, Reduction of nitro aromatic compounds by zero-valent iron metal. Environ. Sci. Technol. 30 (1996), 153-160.

[43] S. Nam, P.G. Tratnyek, Reduction of azo dyes with zero-valent iron. Water Res. 34 (2000), 1837-1845.

[44] X. Zhang, X. Tao, Z. Li, R.S. Bowman, Enhanced perchloroethylene reduction in column systems using surfactant-modified zeolite/zero-valent iron pellets. Environ. Sci. Technol. 36 (2002), 3597-3603.

[45] M.M. Scherer, J.C. Westall, M. Ziomek-Moroz, P.G. Tratnyek, Kinetics of carbon tetrachloride reduction at an oxide-free iron electrode. Environ. Sci. Technol. 31 (1997), 2385-2391.

[46] C. Su, R.W. Puls, Kinetics of trichloroethene reduction by zerovalent iron and tin: Pretreatment effect, apparent activation energy and intermediate products. Environ. Sci. Technol. 33 (1999), 163-168.

[47] V.I. Dubodelov, N.M. Kochegura, S.P. Kazachkov, E.A. Markovskii, V.P. Polishchuk, Effect of the hydrodynamic factor on solution of solid metals in molten metals. Mater. Sci. 8 (1974), 493-495.

[48] J.M. Ottino, Mixing, chaotic advection, and turbulence. Annu. Rev. Fluid Mech. 22 (1990), 207-253.

[49] Noszticzius, Z.; Bodnar, Z.; Garamszegi, L.; Wittmann, M. Hydrodynamic turbulence and diffusion-controlled reactions: simulation of the effect of stirring on the oscillating Belousov-Zhabotinskii reaction with the Radicalator model. J. Phys. Chem. 95 (1991), 6575-6580.

[50] T. Arakaki, A. Mucci, A continuous and mechanistic representation of calcite reaction-controlled kinetics in dilute solutions at 25°C and 1 atm total pressure. Aquat. Geochem. 1 (1995), 105-130.

[51] M.J. Hounslow, H.S. Mumtaz, A.P. Collier, J.P. Barrick, A.S. Bramley, A micro-mechanical model for the rate of aggregation during precipitation from solution. Chem. Eng. Sci. 56 (2001), 2543-2552.

[52] S. Maalej, B. Benadda, Otterbein, M. Influence of pressure on the hydrodynamics and mass transfer parameters of an agitated bubble reactor. Chem. Eng. Technol. 24 (2001), 77-84.

[53] J. Baldyga, L. Makowski, W. Orciuch, Interaction between mixing, chemical reactions, and precipitation. Ind. Eng. Chem. Res. 44 (2005), 5342-5352.

[54] P.E. Dimotakis, Turbulent mixing. Annu. Rev. Fluid Mech. 37 (2005), 329-356.

[55] X. Jiang, Y.G. Zheng; W. Ke, Effect of flow velocity and entrained sand on inhibition performances of two inhibitors for $CO_2$ corrosion of N80 steel in 3% NaCl solution. Corr. Sci. 47 (2005), 2636-2658.

[56] G. Madras, B.J. McCoy, Mixing effects on particle precipitation. Ind. Eng. Chem. Res. 44 (2005), 5267-5274.

[57] P. Polasek, Differentiation between different kinds of mixing in water purification – back to basics, Water SA 33 (2007), 249-252.

[58] S. Nesic, J.K.-L. Lee, A mechanistic model for carbon dioxide corrosion of mild steel in the presence of protective iron. carbonate films—Part 3: film growth model. Corrosion 59 (2003), 616-628.

[59] J. Zhang, N. Li, *Review of studies on fundamental issues in LBE corrosion*. Los Alamos National Labortory 2005.

[60] D.M. Cwiertny, A.L. Roberts, On the nonlinear relationship between kobs and reductant mass loading in iron batch systems. Environ. Sci. Technol. 39 (2005), 8948-8957.

[61] W.A. Arnold, W.P. Ball, A.L. Roberts, Polychlorinated ethane reaction with zero-valent zinc: pathways and rate control. J. Contam. Hydrol. 40 (1999), 183–200.

[62] K.D. Warren, R.G. Arnold, T.L. Bishop, L.C. Lindholm, E.A. Betterton, Kinetics and mechanism of reductive dehalogenation of carbon tetrachloride using zero-valence metals. J. Hazard. Mater. 41 (1995), 217-227.

[63] M. Cohen, The formation and properties of passive films on iron. Can. J. Chem. 37 (1959), 286-291.

[64] U.R. Evans, *Metallic Corrosion, Passivity and Protection*. Longmans, Green & Co., New York, NY, 1948.

[65] H. Klas, H. Steinrath, *The Corrosion of Iron and his Protection* (in German). Stahleisen Düsseldorf, 1974.

[66] M. Stratmann, J. Müller, The mechanism of the oxygen reduction on rust-covered metal substrates. Corros. Sci. 36 (1994), 327-359.

[67] E.J. Caule, M. Cohen, The formation of thin films of iron oxide. Can. J. Chem. 33 (1955), 288-304.

[68] J.F. Devlin, K.O. Allin, Major anion effects on the kinetics and reactivity of granular iron in glass-encased magnet batch reactor experiments. Environ. Sci. Technol. 39 (2005), 1868-1874.

**Table 1**: Effect of shaking speed on the oxidative dissolution of $Fe^0$ in the presence of $2.10^{-3}$ M EDTA (2 mM EDTA). n is the number of experimental points for which the curve iron concentration ([Fe]) vs. time (t) is linear (figure 1). [Fe] = $k_{EDTA}$* t + b; $k_{EDTA}$ and b-values were calculated in Origin 6.0.

| **speed** ($min^{-1}$) | **n** | **r** | $k_{EDTA}$ ($\mu g.h^{-1}$) | **b** ($\mu g$) | $\tau_{EDTA}$ (h) | $\tau_{EDTA}$ (d) |
|---|---|---|---|---|---|---|
| | | | **material A** | | | |
| **0** | 5 | 0.999 | 83 ± 3 | 61 ± 57 | 135 | 5.61 |
| **50** | 7 | 0.980 | 118 ± 11 | 536 ± 226 | 90 | 3.74 |
| **100** | 6 | 0.999 | 135 ± 4 | 926 ± 125 | 76 | 3.17 |
| **150** | 7 | 0.974 | 218 ± 19 | 1096 ± 426 | 46 | 1.93 |
| **200** | 4 | 0.997 | 1775 ± 102 | 771 ± 184 | 6 | 0.24 |
| **250** | 4 | 0.942 | 1970 ± 498 | 3353 ± 1341 | 4 | 0.17 |
| | | | **material B** | | | |
| **50** | 7 | 0.988 | 52 ± 4 | 71 ± 26 | 213 | 8.9 |
| **150** | 7 | 0.995 | 192 ± 9 | 264 ± 77 | 57 | 2.4 |
| **200** | 5 | 0.990 | 898 ± 72 | 758 ± 204 | 12 | 0.5 |
| **250** | 4 | 0.995 | 1070 ± 79 | 415 ± 182 | 10 | 0.42 |

**Table 2:** Some relevant reactions involved in contaminant removal in the system $Fe^0/H_2O$. Ox is the oxidized contaminant and Red its corresponding non or less toxic/mobile reduced form. x is the number of electrons exchanged in the redox couple Ox/Red. It can be seen that $Fe^0$ and its secondary ($Fe^{2+}$, $H/H_2$) and ternary (FeOOH, $Fe_3O_4$, $Fe_2O_3$) reaction products are involved in the process of Ox removal.

| **Reaction equation** | | **Eq.** |
|---|---|---|
| $x\ Fe^0 + Ox_{(aq)}$ | $\Rightarrow Red_{(s\ or\ aq)} + x\ Fe^{2+}_{(aq)}$ | (11) * |
| $2\ Fe^0_{(s)} + O_2 + 2\ H_2O$ | $\Rightarrow 4\ OH^- + 2\ Fe^{2+}_{(aq)}$ | (12) |
| $Fe^0_{(s)} + 2\ H_2O$ | $\Rightarrow H_2 + 2\ OH^- + Fe^{2+}_{(aq)}$ | (13a) |
| $2\ Fe^0_{(s)} + 2\ H_2O + ½\ O_2$ | $\Rightarrow 2\ FeOOH$ | (13b) |
| $x\ H_2 + 2\ Ox_{(aq)}$ | $\Rightarrow 2\ Red_{(s\ or\ aq)} + 2.x\ H^+$ | (14) |
| $x\ Fe^{2+}_{(s\ or\ aq)} + Ox_{(aq)} +$ | $\Rightarrow Red_{(s\ or\ aq)} + x\ Fe^{3+}$ | (15) |
| $2\ Fe^{2+} + ½\ O_2 + 5\ H_2O$ | $\Rightarrow 2\ Fe(OH)_3 + 4\ H^+$ | (16) |
| $Fe(OH)_3$ | $\Rightarrow$ α-, β-FeOOH, $Fe_3O_4$, $Fe_2O_3$ | (17) * |
| $Fe_2O_3 + 6\ H^+ + 2\ e^-$ | $\Rightarrow 2\ Fe^{2+} + 3\ H_2O$ | (18) |
| $Fe_2O_3 + 2\ H^+ + 2\ e^-$ | $\Rightarrow 2\ Fe_3O_4 + H_2O$ | (19) |
| $8\ FeOOH + Fe^{2+} + 2\ e^-$ | $\Rightarrow 3\ Fe_3O_4 + 4\ H_2O$ | (20) |

* non stoichiometric

**Figure 1**

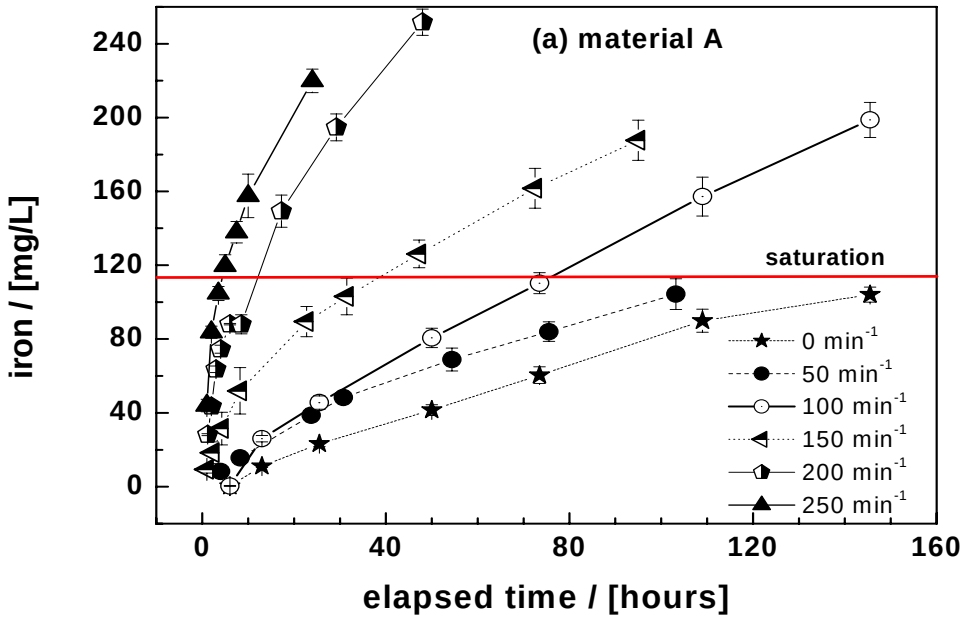
(a) material A
saturation
0 min-1
50 min-1
100 min-1
150 min-1
200 min-1
250 min-1
iron / [mg/L]
elapsed time / [hours]
0
40
80
120
160
200
240

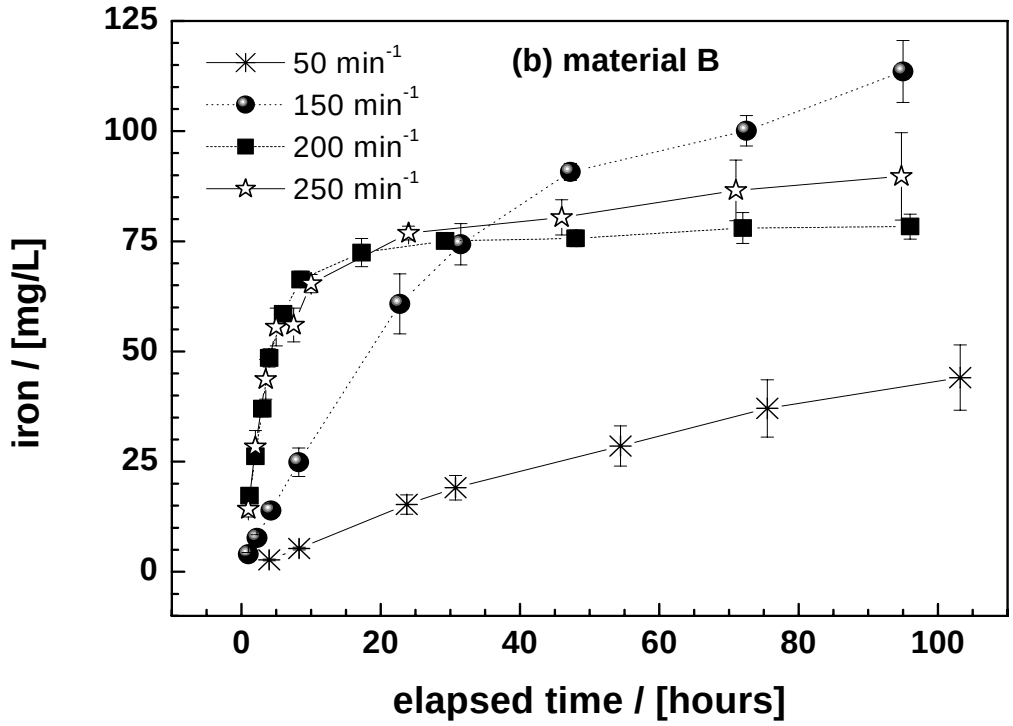
(b) material B
50 min-1
150 min-1
200 min-1
250 min-1
iron / [mg/L]
elapsed time / [hours]
0
25
50
75
100
125
20
40
60
80

**Figure 2**

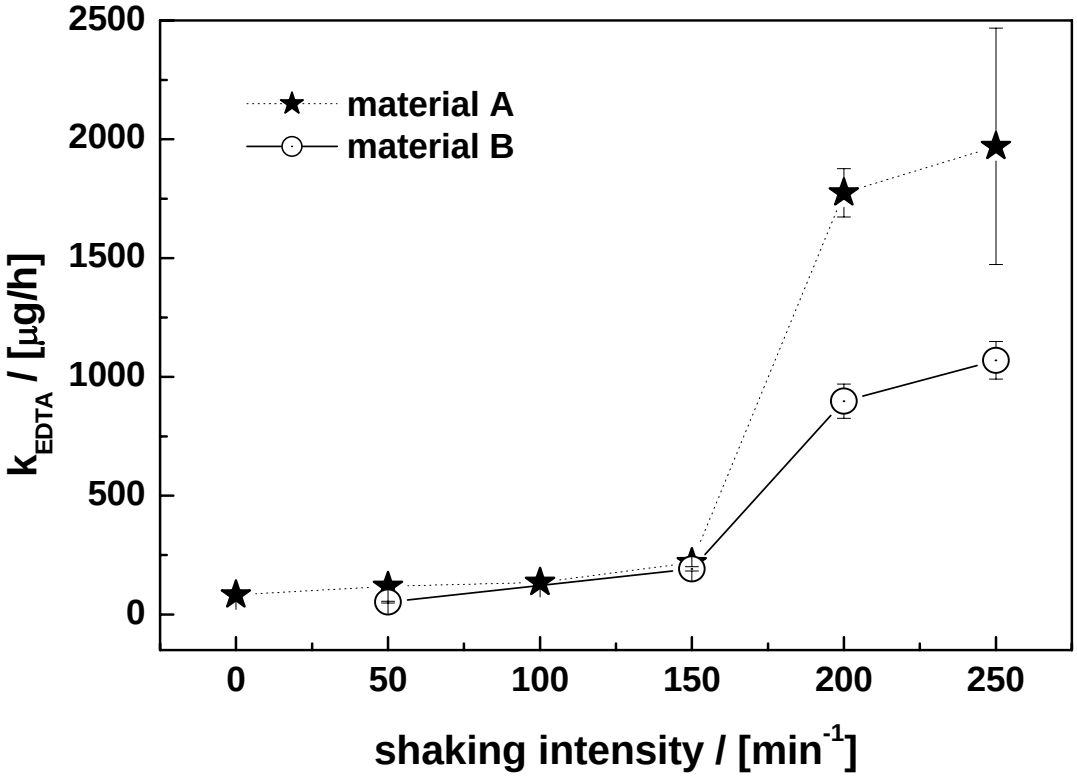
material A
material B
2500
2000
1500
1000
500
0
$k_{EDTA}$ / [µg/h]
0
50
100
150
200
250
shaking intensity / [min$^{-1}$]

**Figure 3**

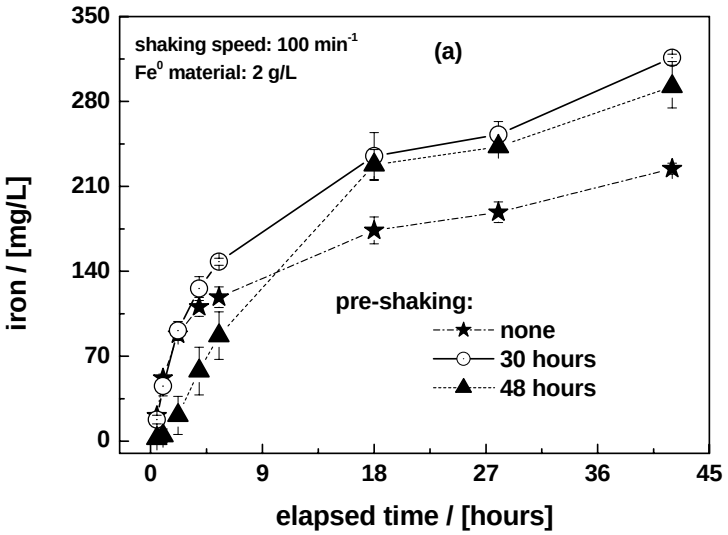
shaking speed: 100 min-1
Fe0 material: 2 g/L
(a)
pre-shaking:
none
30 hours
48 hours
iron / [mg/L]
elapsed time / [hours]
0
70
140
210
280
350
0
9
18
27
36
45

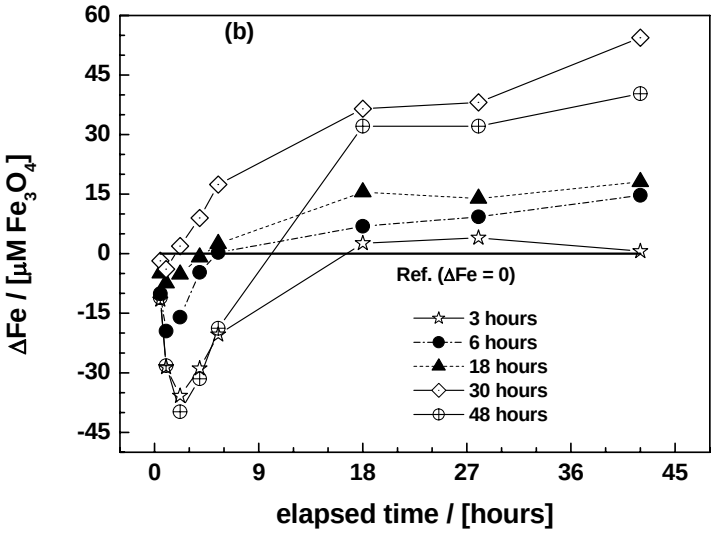
(b)
Ref. (ΔFe = 0)
3 hours
6 hours
18 hours
30 hours
48 hours
ΔFe / [μM Fe3O4]
elapsed time / [hours]
60
45
30
15
0
-15
-30
-45
0
9
18
27
36
45

## Figure Captions

**Figure 1**: Evolution of the total iron concentration as a function of time for different shaking intensities from the scrap iron (a) and the commercial material (b). The experiments were conducted in a 2 mM EDTA solution with a material loading of 2 g/L. The lines are not fitting functions, they simply connect points to facilitate visualization.

**Figure 2**: Variation of the rate of iron dissolution (a values) as a function of the shaking intensity for the scrap iron (material A) and the commercial material (material B). The lines are not fitting functions, they simply connect points to facilitate visualization.

**Figure 3**: Effects of the pre-shaking time on the iron dissolution in 0.115 M ascorbate buffer (pH 7.6): (a) kinetics of iron dissolution in the reference system and the systems pre-shaken for 30 and 48 hours; (b) excess iron amount ($\Delta$Fe) as function of the time in all systems in comparison to the reference system. The lines are not fitting functions, they simply connect points to facilitate visualization.